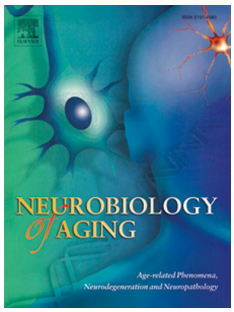

Choroid Plexus Volume is Associated With Levels of CSF Proteins: Relevance for Alzheimer's and Parkinson's Disease

Ehsan Tadayon, M.D., Alvaro Pascual-Leone, M.D., Ph.D., Daniel Press, M.D., Emiliano Santarnecchi, Ph.D., for the Alzheimer's Disease Neuroimaging Initiative

PII: S0197-4580(20)30013-0

DOI: https://doi.org/10.1016/j.neurobiolaging.2020.01.005

Reference: NBA 10756

To appear in: *Neurobiology of Aging*

Received Date: 16 May 2019

Revised Date: 6 January 2020

Accepted Date: 13 January 2020

Please cite this article as: Tadayon, E., Pascual-Leone, A., Press, D., Santarnecchi, E., for the Alzheimer's Disease Neuroimaging Initiative, Choroid Plexus Volume is Associated With Levels of CSF Proteins: Relevance for Alzheimer's and Parkinson's Disease, *Neurobiology of Aging* (2020), doi: https://doi.org/10.1016/j.neurobiolaging.2020.01.005.

Choroid Plexus Volume is Associated With Levels of CSF Proteins: Relevance for Alzheimer's and Parkinson's Disease

Ehsan Tadayon, M.D.[1], Alvaro Pascual-Leone, M.D., Ph.D.[1-2], Daniel Press, M.D.[1], Emiliano Santarnecchi, Ph.D.[1], for the Alzheimer's Disease Neuroimaging Initiative*

[1] *Berenson-Allen Center for Non-Invasive Brain Stimulation and Division for Cognitive Neurology, Beth Israel Deaconess Medical Center, Harvard Medical School, Boston, MA, USA*
[2] *Institut Universitari de Neurorehabilitacio Guttmann, Badalona, Barcelona, Spain*

*Data used in the preparation of this article were obtained from the Alzheimer's Disease Neuroimaging Initiative (ADNI) database (adni.loni.usc.edu). As such, the investigators within the ADNI contributed to the design and implementation of ADNI and/or provided data but did not participate in analysis or writing of this report. A complete listing of ADNI investigators can be found at: http://adni.loni.usc.edu/wpcontent/uploads/how_to_apply/ADNI_Acknowledgement_List.pdf

Running title: Choroid plexus and CSF proteins

Title word count: 18

Abstract word count: 162

Body word count (summary, introduction, methods, results, discussion): 3083

Figures: 4

Tables: 2

Supplemental Information: 3 tables, 3 Figures

Financial disclosures: All authors report no conflict of interest

Corresponding author:

Ehsan Tadayon, M.D. and Emiliano Santarnecchi, Ph.D

Berenson-Allen Center for Non-Invasive Brain Stimulation, Beth Israel Deaconess Medical Center,

Harvard Medical School, Boston, MA, USA

Phone:617-516-9516

emails: stadayon@bidmc.harvard.edu ; esantarn@bidmc.harvard.edu

Summary

The Choroid plexus (ChP) is a major source of cerebrospinal fluid (CSF) production, with a direct and indirect role in protein clearance, and pathogenesis of Alzheimer's disease (AD). Here, we tested the link between the ChP volume and levels of CSF proteins in two datasets of (i) healthy controls, mild cognitive impairment (MCI) and AD patients from the Alzheimer's Disease Neuroimaging Initiative (ADNI) (N = 509), and (ii) healthy controls and Parkinson's disease (PD) patients from the Parkinson's Progression Markers Initiative (PPMI) (N=302). All subjects had baseline CSF proteins (amyloid-β, total and phosphorylated-tau and α-synuclein (only in PPMI)). ChP was automatically segmented on 3T structural T1-weighted MRIs. We found negative associations between ChP volume and CSF proteins, which was stronger in healthy controls, early-MCI and PD compared with late-MCI and AD. Further grouping of subjects into amyloid-positive and negative based on their florbetapir (AV45) PET imaging showed that the association between ChP and CSF proteins was lower in amyloid-positive group. Our findings support the possible role of ChP in the clearance of CSF proteins, provide evidence for ChP dysfunction in AD and suggest the need to account for the ChP volume in future studies of CSF-based biomarkers.

Keywords:

Choroid plexus, CSF proteins, CSF clearance, Alzheimer's disease, Parkinson's disease

Abbreviations:

MRI: Magnetic Resonance Imaging

AD: Alzheimer's disease

PD: Parkinson's disease

ChP: choroid plexus

CSF: cerebrospinal fluid

EMCI: early-mild cognitive impairment

LMCI: late-mild cognitive impairment

SMC: significant memory concern

1. Introduction

Many neurodegenerative disorders are pathologically characterized by the aberrant deposition of protein aggregates within the brain parenchyma. In Alzheimer's disease (AD), amyloid-β (Aβ) plaques and neurofibrillary tangles are the pathognomonic pathological features (Perl, 2010). Historically, protein deposition was attributed to the increased production of aberrant proteins in the brain; however, recent studies have found that dysfunctional brain clearance systems contribute significantly to protein deposition. In AD, a lower amount of Aβ clearance has been shown compared to healthy controls, while the amount of Aβ production was not different (Mawuenyega et al., 2010). This has prompted investigations on the various brain clearance systems, with possible therapeutic implications in AD (Tarasoff-Conway et al., 2015). Many of the newly found clearance systems such as the glymphatic system require cerebrospinal fluid (CSF) for their functionality (Jessen et al., 2015). Thus, derangements in CSF production can potentially contribute to protein deposition in neurodegenerative disorders.

The majority of CSF is produced in a delicate epithelial-endothelial structure, called choroid plexus (ChP) (Damkier et al., 2013), which extends along the floor of the lateral ventricles and the roof of the third and fourth ventricles (**Figure 1A**) (Benarroch, 2016). In addition, ChP can directly clear CSF proteins via rich transporters and receptors lining its epithelial surface (Alvira-Botero and Carro, 2010; Crossgrove et al., 2005; Fujiyoshi et al., 2011). This suggests both an indirect and a direct role of ChP in the pathogenesis of neurodegenerative disorders such as AD. Animal studies have shown ChP pathological changes in AD, possibly interfering with its function in CSF

production and brain clearance (Alvira-Botero and Carro, 2010). Investigating the ChP structure and function can provide insight into its possible role in protein clearance and pathogenesis of neurodegenerative disorders.

Assuming larger ChP is associated with higher CSF production as well as larger number of CSF-blood protein transporters, we first sought to assess if a negative association between the ChP volume and levels of CSF proteins can be found. We sought to examine this hypothesis in two large cohorts of (i) healthy controls, mild cognitive impairment (MCI), and AD and (ii) healthy controls and PD. CSF proteins have been increasingly used as diagnostic and prognostic biomarkers in various neurological disorders as they reflect the underlying brain pathology. In AD, the core CSF proteins' profile includes Aβ, total-tau (t-tau), and phosphorylated-tau (p-tau), which reflect key aspects of disease pathogenesis, including extracellular Aβ plaque deposition, intracellular tangle formation and neuronal degeneration (Blennow et al., 2010). While changes in t-tau and p-tau levels occur late in AD, changes in Aβ occur early in the course of the disease, therefore, Aβ changes can potentially reflect clearance dysfunction in MCI/AD (Jack and Holtzman, 2013). CSF proteins are also actively being investigated in Parkinson's Disease (PD) (Andersen et al., 2017). In addition to the core AD CSF proteins, CSF α-synuclein (α-syn) has been studied as a potential diagnostic and prognostic biomarker of PD (Hong et al., 2010). We first assessed the association between the ChP volume and each CSF protein separately and as the levels of different CSF proteins are correlated, we also used a statistical approach to find an association between the ChP volume and the correlated variation among CSF proteins. Next, we examined whether the association between the ChP volume and CSF proteins would be

lower in AD compared to other diagnostic groups. Moreover, as the accumulation of Aβ occur early in the course of AD, heralding a possible clearance dysfunction, we grouped participants into amyloid-positive and amyloid-negative based on their florbetapir Positron Emission Tomography (PET) imaging to test whether the relation between the ChP volume and CSF proteins would be lower in amyloid-positive group. Details on the study design, data and methods are provided, with a discussion on the potential implications of the present findings and future directions.

2. Methods

2.1 Study design

We examined the link between the ChP volume and CSF protein levels in two large cohorts. The first cohort included healthy controls, subjects with significant memory concern (SMC), early-mild cognitive impairment (EMCI), late-mild cognitive impairment (LMCI) and AD patients from the Alzheimer's Disease Neuroimaging Initiative (ADNI) database. The ADNI was launched in 2003 as a public-private partnership, led by Principal Investigator Michael W. Weiner, MD. The primary goal of ADNI has been to test whether serial MRI, PET, other biological markers, and clinical and neuropsychological assessment can be combined to measure the progression of MCI and early AD. Our study population consisted of healthy controls, individuals with SMC (which were combined with healthy controls throughout the study), EMCI, LMCI, and AD from ADNI-2 who had baseline high-resolution 3T structural T1 MRIs and CSF measures (t-tau, p-tau, and Aβ). Data used in this study were obtained from adni.loni.usc.edu.

The second cohort included healthy controls and Parkinson's disease (PD) patients from the Parkinson's Progression Markers Initiative (PPMI) dataset. PPMI is a collaborative clinical and biomarker study of patients with PD and healthy controls. Our study population consisted of healthy controls and newly diagnosed, treatment-naïve PD subjects who had baseline 3T structural T1-weighted MRIs and CSF measures (t-tau, p-tau, Aβ, and α-syn). For further information on the study, visit www.ppmi-info.org.

2.2 Imaging data and analysis

2.2.1 Structural T1-weighted MRIs

3T T1-weighted MRIs were downloaded from ida.loni.usc.edu website for PPMI and ADNI-2 cohorts. For a detailed description of MRI protocols see ppmi-info.org and adni.loni.usc.edu. Automated segmentation of ChP within the lateral ventricles was performed using Freesurfer software package (http://surfer.nmr.mgh.harvard.edu/), which has been previously utilized for segmenting ChP from structural MRIs (Baker et al., 2017; Zhou et al., 2015). We used the Freesurfer subcortical segmentation output aseg.mgz for further analyses. We combined voxels segmented as left and right ChP (indexed as 31 and 63 in aseg.mgz) to get a single ChP mask. To ensure that the association between ChP volume and CSF proteins is not driven by other confounding factors, we also measured ventricular volume (by combining left and right lateral ventricles (aseg indices: 4 and 43), left and right inferior lateral ventricles (aseg indices: 5 and 44), third ventricle (aseg index: 14) and fourth ventricle (aseg index: 15)), as well as cortical grey matter volume (aseg indices: 3 and 42).

2.2.2 PET imaging

For florbetapir (AV45) PET data, we used average AV45 standard uptake value ratio (SUVR) of frontal, anterior cingulate, precuneus, and parietal cortex relative to the cerebellum provided by the ADNI (https://ida.loni.usc.edu/). We grouped participants into amyloid-positive and negative using SUVR≥1.11 (Landau et al., 2013; Schreiber et al., 2015) (See also Supplementary Figure 3).

2.3 CSF proteins

In the ADNI-2 cohort, CSF was collected from all subjects at baseline and every two years. Only CSF proteins measured at baseline were used for the purpose of this study. CSF Aβ, t-tau and p-tau (phosphorylated at the threonine 181 position) were measured using electrochemiluminescence immunoassays on a fully automated Elecsys cobas e 601 instrument at the UPenn/ADNI Biomarker Laboratory. For this study, we used data from UPENNBIOMK9_04_19_17.csv available on LONI website.

In the PPMI cohort, CSF was collected from all subjects at baseline and every six months. Only CSF proteins measured at baseline were used for the purpose of this study. Three CSF biomarkers including Aβ, t-tau, and p-tau (phosphorylated at the threonine 181 position) were measured using the multiplex xMAP Luminex platform and Innogenetics immunoassay kits. CSF α-syn was measured using a commercially available enzyme-linked immunosorbent assay kit (Covance). Detailed description regarding CSF preparation and analysis can be found at ppmi-info.org.

Levels of CSF proteins are correlated with each other. To test whether ChP volume contributes to the shared variance between CSF proteins, we applied principal component analysis (PCA) to capture the correlated variation in CSF proteins. PCA is a statistical technique that decomposes the data into uncorrelated components. Each component is a weighted sum (loadings) of initial features (here, CSF proteins). The first principal component (PC1) captures the highest amount of variance, while the second component is orthogonal (uncorrelated) to the first component and accounts for the second-largest amount of variance, and so on. We tested the association between ChP volume and PC1 scores as it accounted for a large portion of variance in CSF proteins.

2.4 Statistical analysis

Histograms of CSF protein levels were visually inspected. Due to the highly skewed distribution of CSF proteins, all CSF protein levels were log-transformed for both the ADNI and PPMI cohorts. We tested the association between CSF proteins (dependent variables) and age, sex, APOEε4 status, diagnostic group, cortical volume, ventricular volume, and the ChP volume in univariate linear regression analyses and multivariate linear regression analyses. We also performed two additional multiple regression analyses to control for total brain volume (TBV). The first analysis included TBV as a covariate and the second analysis normalized brain volumes by TBV. The results for these two models can be found in Supplementary Table 2 and 3. To check for the assumptions of linear regression and potentially rectify them, we visually inspected the four main plots of (i) Residuals vs. Fitted (to check for linear assumption) (ii) Normal Q-Q plot (to check for normality) (iii) Scale-Location plot (to check for homoscedasticity) and (iv) Residuals vs Leverage plot (to check for influential outliers using Cook's distance). We also used the Shapiro test to check for normality of residuals. We didn't find any violation of linear regression assumptions and none of the models were influenced by an influential outlier (measured by Cook's distance). For multiple regression models, we used the Variance Inflation Factor (VIF) to check for possible collinearity (VIF > 4 was considered as possible collinearity). PCA was applied to the CSF proteins in each dataset and the scores were computed by projecting data onto the corresponding component. Partial correlation between ChP volume and PC1 was used while we controlled for the confounding covariates. The amount of variance in CSF proteins explained by ChP volume was measured in each diagnostic group

separately by comparing the R^2 of the model that included age, sex, APOEε4, and cortical volume (ChP- model) with the model that included age, sex, APOEε4, cortical volume and ChP volume (ChP+ model). F-test was used to compare the two models ($p<0.01$ was deemed statistically significant). 1000 bootstrap samples were generated (with replacement) and the change in R2 (ΔR^2) was measured between ChP+ and ChP- models across all the samples to find the confidence interval for ΔR^2. To test whether being amyloid-positive would change the association between ChP volume and t-tau/p-tau, we fitted a linear regression model including age, sex, APOEε4, cortical volume, ventricular volume, ChP volume, amyloid-positive, and the interaction terms between amyloid-positive and brain volumes (cortical volume, ChP volume, ventricular volume). We tested whether the amyloid-positive and ChP volume interaction was significant. For the purpose of visual presentation, we used partial correlation to show the correlation between ChP volume and t-tau/p-tau for amyloid-positive and amyloid-negative groups separately, while we controlled for age, sex, APOEε4, cortical volume, and ventricular volume. To compare the predictive value of the ChP volume, cortical volume, and ventricular volume, we separately added each to a model that included age, sex, group and APOEε4 (basic model) and measured adjusted R^2. One-way ANOVA followed by the Tukey test to control for multiple comparisons was used to check for differences in the ChP volume between diagnostic groups. Python and R were used for the statistical analyses.

3. Results

3.1 Demographic information, CSF biomarkers, and imaging

Table 1 shows the demographic information (including age, gender, and APOEε4 status), levels of CSF biomarkers, brain volumes (including TBV, cortical volume, ventricular volume, and the ChP volume) for both the ADNI and PPMI datasets, and florbetapir (AV45) PET imaging SUVR values for the ADNI dataset.

3.2 ChP segmentation

Figure 1B shows the segmented ChP for three example subjects. There was a statistically significant difference between groups as determined by a one-way ANOVA test ($F_{(6,776)}$ = 7.98, p-value = $2.27x10^{-8}$). A Tukey post hoc test revealed that AD patients had larger ChP volume compared with other diagnostic groups ($p<0.05$).

3.3 Association between ChP volume and CSF proteins

Supplementary Table 1 provides results for univariate regression analyses to predict CSF proteins using age, sex, APOE ε4, diagnostic group, cortical volume, ventricular volume, and ChP volume as independent variables. ChP volume was negatively correlated with CSF proteins across both datasets ($p < 0.01$). In multivariate analyses, ChP volume showed significant association with t-tau (β = - 0.33, $p < 0.001$) and p-tau (β = -0.34 , $p < 0.001$) in ADNI-2, as well as t-tau (β = -0.24, $p < 0.001$), α-syn (β = - 0.24, $p < 0.001$) and Aβ (β = -0.1 , $p < 0.001$) in PPMI (**Table 2**). The associations between ChP volume and p-tau in PPMI and Aβ in ADNI-2 were not statistically

significant (p =0.09, p=0.03 respectively). VIF was less than two for all the tested models (no collinearity).

CSF proteins showed a positive correlation with each other in both the ADNI and PPMI datasets (Supplementary Figures 1 and 2). To capture the shared variance between CSF proteins, PCA was applied (Figure 2A and 2D). The first principal component (PC1) explained around 60 percent of the variance in CSF proteins in both the ADNI and PPMI datasets (Figure 2B and 2E). In PPMI, all CSF proteins had positive loadings in PC1 (i.e. all CSF proteins were positively correlated with each other). In ADNI, t-tau and p-tau showed the highest loadings in PC1, while Aβ had loading near zero. Figure 2C and Figure 2F show partial correlation of ChP volume and PC1 after controlling for age, sex, APOEε4 status, diagnostic group, and cortical volume ($r_{partial} = -0.43$ ($p < 0.001$) in PPMI and $r_{partial} = -0.40$ ($p < 0.001$) in ADNI-2).

3.4 Association between ChP volume and CSF proteins is lower in AD

We examined the amount of variance explained by ChP volume in each diagnostic group separately. In ADNI, the amount of variance in CSF proteins explained by ChP volume was higher in healthy controls and EMCI compared to LMCI and AD (**Figure 3A**), while the ChP volume explained a similar amount of variance in CSF proteins in healthy controls and PD patients (**Figure 3B**).

3.5 Florbetapir amyloid-positive subjects have lower association between the ChP volume and t-tau/p-tau

In ADNI, participants were grouped into amyloid-positive and amyloid-negative based on their florbetapir (AV45) PET imaging SUVR (AV45>= 1.11) (Table 1). The multiple linear regression models showed a trend that amyloid-positive reduced the association between ChP volume and CSF proteins (for t-tau: β_{ChP} = -0.32, p-value < 0.001 and $\beta_{interaction}$ = 0.09, p-value = 0.07; for p-tau: β_{ChP} = -0.25, p-value < 0.001 and $\beta_{A\beta + x\ ChP}$ = 0.12, p-value = 0.04). Importantly, the interaction term ($\beta_{A\beta+ x\ ChP}$) was positive, which indicates that the negative association between ChP volume and CSF proteins (β_{ChP}) is less in amyloid-positive patients. Figure 5 shows the partial correlation between ChP volume and t-tau/p-tau in amyloid-positive and amyloid-negative groups, controlled for the confounding variables.

3.6 Cortical volume, ventricular volume and CSF proteins

Cortical volume did not show any significant association with CSF proteins in univariate analyses of PPMI data, whereas it was negatively associated with t-tau/p-tau and positively associated with Aβ in ADNI-2 cohort (**Supplementary Table 1**). Multivariate analyses only showed a significant association between cortical volume and Aβ in PPMI (**Table 2**). In univariate regression analysis, ventricular volume showed negative associations with t-tau, α-syn, p-tau, and Aβ in PPMI and only with Aβ in ADNI-2 (Supplementary Table 1). In multivariate regression analyses, the associations between CSF proteins and ventricular volume were not statistically significant except for p-tau in PPMI and Aβ in ADNI-2 (**Table 2**).

Cortical volume showed a weak correlation with ChP volume in PPMI ($r = 0.12$, $p < 0.05$) and ADNI-2 ($r = 0.16$, $p < 0.001$), while ventricular volume was positively correlated with the ChP volume across the two cohorts ($r \sim 0.63$, $p < 10^{-3}$) (**Figure 4B**). To compare the predictive value of cortical, ventricular and ChP volume, we separately added each predictor to a model including age, sex, APOEε4 status, and diagnostic group to predict CSF proteins (basic model) (**Figure 4C**). The model that included ChP volume showed higher adjusted R^2 compared to the models that included cortical volume or ventricular volume for Aβ, p-tau, and t-tau in the ADNI and Aβ, t-tau and α-syn in PPMI.

4. Discussion

We examined the association between the ChP volume and CSF proteins in a large cohort of healthy controls, SMC, EMCI, LMCI and AD patients (ADNI cohort), and healthy controls and PD patients (PPMI cohort). We found a negative association between the ChP volume and levels of each tested CSF protein in both univariate and multivariate regression analyses. To account for the positive correlation between CSF proteins, we applied PCA to capture the shared variance in CSF proteins and found that the ChP volume had a negative association with the first principal component (PC1). We then showed that the association between the ChP volume and levels of CSF proteins was highest in healthy controls and EMCI patients, with a lower association in LMCI and AD groups in the ADNI cohort. On the other hand, ChP volume showed similar association with levels of CSF proteins in healthy controls and PD patients in the PPMI cohort. Using florbetapir PET imaging data, we grouped participants into amyloid-

positive and amyloid-negative and found that the association between ChP volume and t-tau/p-tau was lower in amyloid-positive group. We finally demonstrated that ChP volume had a stronger association with CSF proteins compared to ventricular volume and cortical volume. Our results are in line with prior animal and in vitro studies and suggest a possible role of ChP in the clearance of CSF proteins, support possible ChP dysfunction in AD and highlight ChP volume as a contributing factor to inter-individual variance in levels of CSF proteins.

We hypothesized that larger ChP volume would be associated with lower levels of CSF proteins for two reasons: (i) indirectly through higher production of CSF proteins and (ii) directly by providing larger number of CSF-blood protein transporters on the ChP epithelial tissue. Although no study has been performed to show the relationship between ChP volume and the amount of CSF secretion, there are lines of evidence in favor of this hypothesis. For instance, choroid plexus papillomas (CPP) are benign congenital intracranial tumors that are mostly found in the lateral ventricles and one of its major complications is hydrocephalus. One major mechanism behind CPP's hydrocephalus is overproductions of CSF from the choroid plexus tissue(RR, 2003; Sachan, 2017). Thus, it can indirectly be inferred that larger ChP volume can lead to increased CSF production through increased number of functional units. Increased CSF production can enhance the activity of CSF-dependent brain clearance systems. For instance, the newly described glymphatic pathway starts with CSF entry into the brain via periarterial spaces with entrance into interstitium via aquaporin-4 water channels expressed on astrocytes (Jessen et al., 2015). This creates a convective current that drives interstitial fluid into perivenous spaces and clear brain of waste products such as

Aβ (Iliff et al., 2012). Once inside the CSF, waste products are absorbed into the circulatory or lymphatic systems.

Furthermore, recent molecular studies have attributed new functionalities to ChP, highlighting its direct role in clearing CSF proteins. To that end, two conditions should be met: (i) proteins produced in the brain should be able to enter ventricles adjacent to choroid plexus and (ii) choroid plexus should be able to capture these proteins. As for the former, studies using horseradish peroxidase and fluorescent tracers injected into brain parenchyma have shown entrance of tracers into lateral ventricles mainly via interstitial fluid (ISF) bulk flow after passing through ependymal layer (Bedussi et al., 2015; Cserr et al., 1977), supporting the idea that brain-derived proteins can enter lateral ventricles adjacent to ChP. Moreover, molecular studies of ChP epithelial cells have revealed many transporters on the apical side of the epithelium responsible for transporting proteins. For instance, many of the Aβ transporters (such as LRP1, LRP2, RAGE, ABCB1) that are normally expressed at the Blood-Brain Barrier (BBB) have been also localized on ChP epithelium on the CSF side (Crossgrove et al., 2005). One study showed that radiolabeled Aβ ([^{125}I]hAβ(1-40)) injected into rat's lateral ventricles are taken up by ChP and removed from CSF five times faster if it was only removed via CSF bulk flow, further emphasizing the direct role of ChP in clearing CSF proteins (Fujiyoshi et al., 2011).

Previous animal studies have shown pathological changes of ChP in AD, possibly leading to ChP dysfunction (Balusu et al., 2016; Krzyzanowska and Carro, 2012). This has led some groups to test the therapeutic role of ChP epithelial stem cells in AD treatment with promising results (Aliaghaei et al., 2015; Bolos et al., 2014). In line

with animal studies, we found dissociation between the amount of CSF proteins explained by ChP volume across AD spectrum disorders, with a stronger association in healthy controls and EMCI groups compared to LMCI and AD patients. CSF proteins in healthy controls and PD patients showed more or less similar association with ChP volume, possibly suggesting a disease-specific role of ChP in AD. As Aβ accumulates early in the disease (before any apparent cognitive changes or changes in t-tau and p-tau levels)(Jack and Holtzman, 2013), we furthered our analyses by grouping the ADNI subjects into amyloid-positive and negative based on their florbetapir PET imaging data. We found that amyloid-positive subjects had lower association between ChP volume and t-tau and p-tau compared with amyloid-negative subjects. However, future studies with larger sample sizes and robust imaging techniques for measuring CSF production and clearance dysfunction are needed to causally evaluate if Aβ accumulation precedes ChP dysfunction.

Prior studies have suggested a possible association between brain volumetric measurements and CSF proteins; however, these studies have mainly focused on ventricular volume while largely ignoring ChP volume as a possible factor explaining the inter-individual difference of CSF proteins. In a study of healthy controls and AD patients, Ott et al. (Ott et al., 2010) reported a negative association between ventricular volume and CSF t-tau in AD subjects. More recently, in a study of 730 healthy controls, MCI and AD subjects, a negative association was found between ventricular volume and Aβ, while the association for t-tau and p-tau was not significant (van Waalwijk van Doorn et al., 2017). In another recent study, ventricular volume showed a negative association with Aβ-38 and Aβ-40 with no significant association with t-tau, p-tau and

Aβ-42 (Edsbagge et al., 2017). Two main hypotheses can explain the possible association between ventricular volume and CSF proteins. The first hypothesis argues that disease severity can explain the negative association between Aβ and ventricular volume as CSF Aβ declines while ventricular volume increases with disease severity. Based on this hypothesis, one would expect to find a positive correlation between ventricular volume and t-tau/p-tau, as CSF concentrations of these proteins increase with disease severity as well (Sämgård et al., 2010). However, previous studies have either found negative associations between ventricular volume and t-tau and p-tau, or no association at all. The second hypothesis argues for the dilutional effect of increased ventricular volume, predicting a negative correlation between various CSF proteins and ventricular volume. Although the dilutional effect of ventricular volume cannot be rejected, our results show a stronger association between CSF proteins/ChP volume compared to CSF proteins/ventricular volume. Given that the ChP volume and ventricular volume show a significant correlation, previously observed associations between ventricular volume and CSF proteins, albeit weak, could be explained –and reinterpreted— by ChP volume.

Lastly, levels of CSF proteins were positively correlated with each other. The association between t-tau and Aβ is important to note as previous studies have shown a complex and nonlinear dynamic association between the two in AD (de Leon et al., 2018). This can raise the question how the ChP volume can be negatively correlated with both t-tau and Aβ. To answer this concern, we showed that Aβ and t-tau had positive association in both healthy controls and PD patients in PPMI, as well as healthy controls of the ADNI (Supplementary Figures 1 and 2). The direction of the association

changed to negative in the EMCI and the LMCI groups, with no association in the AD group. This confirmed the dynamic nature of correlation between Aβ and t-tau in the EMCI/LMCI/AD groups. To account for the correlated variation between CSF proteisn, we performed PCA. We were able to show that ChP volume is associated with the first principal component (PC1), which explained about 60% of the variance in levels of CSF proteins. Together, these suggest that ChP volume is a contributing factor to all the CSF proteins, which can account for the shared variance between the CSF proteins. The ChP contribution is more pronounced in healthy controls, EMCI and PD patients and lower in LMCI and AD.

5. Study limitations and future directions

In the present study, we indirectly measured the volume of ChP from structural T1-weighted MRIs. The gold-standard technique to non-invasively visualize ChP is T1-weighted MRIs enhanced with contrast. The fenestrated endothelium in ChP allows contrast to accumulate in the interstitium, while the ChP-CSF barrier precludes contrast to leak into the CSF (Shi et al., 2017). However, contrast-enhancing agents are not used in research studies routinely and their usage is mainly limited to clinical settings where the benefits outweigh their risks. On the other hand, high-resolution T1-w MRIs are routinely acquired in research studies, where ChP has intensity similar to grey matter voxels. T1-weighted MRIs can be utilized to study ChP within lateral ventricles, which have the largest ChP among all brain ventricles. However, they do not have enough resolution for segmenting ChP within third and fourth ventricles. New MRI

sequences, as well as 7T anatomical MRIs, could provide better resolution to study ChP within third and fourth ventricles without the need to use contrast-enhancing agents.

Although ChP within lateral ventricles can be manually segmented, it precludes large-scale neuroimaging studies given its time-consuming nature. This highlights the need for accurate automatic ChP segmentation techniques. Freesurfer software has been used in the majority of previous studies for automatic ChP segmentation; however, future studies are needed to accurately measure its accuracy. Moreover, new algorithms that are developed solely to segment ChP could be beneficial in studying the structure and function in large-scale neuroimaging studies. It is important to note that ChP can undergo calcification that might affect the segmentation accuracy. Although generally considered benign, future studies are needed to study if ChP calcification can lead to ChP dysfunction and if it can impact ChP volumetric measurements.

We found that the ChP volume was larger in AD compared to other groups. Although the difference in the ChP volume was statistically significant between AD and other groups, the effect size is minimal. Several factors could explain the observed larger ChP volume in AD. Given that ventricles are enlarged in AD patients, this could lead to the overestimation of ChP segmentation due to automatic segmentation inaccuracy. Reduced pressure in ventricles as a result of ventricular enlargement can also lead to apparent ChP enlargement in AD.

Aside from measuring ChP volume, new techniques can be used to obtain information about the structural and functional properties of ChP. MRI techniques such as Arterial Spin Labeling (ASL) might provide important information regarding ChP perfusion, given its highly vascular stroma and substantial blood perfusion relative to the

brain parenchyma (Dangouloff-Ros et al., 2015). In addition, developing new techniques that allow non-invasive measurement of CSF production rate as well as assessing glymphatic system efficiency can open new windows into identifying patients at risk of developing AD as well as disease prognosis (Harrison et al., 2018).

6. Conclusion

We found a negative association between the ChP volume and levels of CSF proteins. Moreover, we showed that the association between ChP volume and CSF proteins is low in LMCI and AD groups compared with healthy controls, EMCI and PD. Our results support a potential role of ChP in CSF protein clearance and support prior animal studies showing ChP dysfunction in AD. Our results also introduce ChP volume as a factor contributing to the variability in levels of CSF proteins and suggest the importance of accounting for ChP volume in future studies of CSF-based biomarkers.

Acknowledgments

We would like to thank Dr. Lucia Monti, Francesco Neri and Lucia Mencarelli for collecting T1-weighted MRI data with contrast for the validation study. This work was conducted with support from Harvard Catalyst | The Harvard Clinical and Translational Science Center (National Center for Advancing Translational Sciences, National Institutes of Health Award UL 1TR002541) and financial contributions from Harvard University and its affiliated academic healthcare centers. The content is solely the responsibility of the authors and does not necessarily represent the official views of Harvard Catalyst, Harvard University and its affiliated academic healthcare centers, or the National Institutes of Health. Data collection and sharing for this project was funded by the Alzheimer's Disease Neuroimaging Initiative (ADNI) (National Institutes of Health Grant U01 AG024904) and DOD ADNI (Department of Defense award number W81XWH-12-2-0012). ADNI is funded by the National Institute on Aging, the National Institute of Biomedical Imaging and Bioengineering, and through generous contributions from the following: AbbVie, Alzheimer's Association; Alzheimer's Drug Discovery Foundation; Araclon Biotech; BioClinica, Inc.; Biogen; Bristol-Myers Squibb Company; CereSpir, Inc.; Cogstate; Eisai Inc.; Elan Pharmaceuticals, Inc.; Eli Lilly and Company; EuroImmun; F. Hoffmann-La Roche Ltd and its affiliated company Genentech, Inc.; Fujirebio; GE Healthcare; IXICO Ltd.; Janssen Alzheimer Immunotherapy Research & Development, LLC.; Johnson & Johnson Pharmaceutical Research & Development LLC.; Lumosity; Lundbeck; Merck & Co., Inc.; Meso Scale Diagnostics, LLC.; NeuroRx Research; Neurotrack Technologies; Novartis Pharmaceuticals Corporation; Pfizer Inc.; Piramal Imaging; Servier; Takeda Pharmaceutical Company; and Transition Therapeutics. The Canadian Institutes of Health Research is providing funds to support ADNI clinical sites in Canada. Private sector contributions are facilitated by the Foundation for the National Institutes of Health (www.fnih.org). The grantee organization is the Northern California Institute for Research and Education, and the study is coordinated by the Alzheimer's Therapeutic Research Institute at the University of Southern California. ADNI data are disseminated by the Laboratory for Neuro Imaging at the University of Southern California.

Author contributions

ET designed the study, analyzed the data and wrote the manuscript. APL edited the manuscript and supervised the study. ES supervised the study, and wrote the manuscript.

Conflicts of interest

All authors report no conflict of interest.

Funding

ES and APL are supported by the BROAD Institute at Harvard-MIT (Boston, MA, USA) via 2016P000351. ES and APL are partially supported by Defense Advanced Research Projects Agency (DARPA) via HR001117S0030. ES is supported by the Beth Israel Deaconess Medical Center (BIDMC) via the Chief Academic Officer (CAO) grant 2017. APL is further supported by the Berenson-Allen Foundation, the Sidney R. Baer Jr. Foundation, grants from the National Institutes of Health (R01HD069776, R01NS073601, R21 MH099196, R21 NS082870, R21 NS085491, R21 HD07616), and Harvard Catalyst, The Harvard Clinical and Translational Science Center (NCRR and the NCATS NIH, UL1 RR025758). The content of this paper is solely the responsibility of the authors and does not necessarily represent the official views of Harvard Catalyst, Harvard University and its affiliated academic health care centers, the National Institutes of Health, the Sidney R. Baer Jr. Foundation.

References

Aliaghaei, A., Digaleh, H., Khodagholi, F., Ahmadiani, A., 2015. Encapsulated Choroid Plexus Epithelial Cells Actively Protect Against Intrahippocampal Aβ-induced Long-Term Memory Dysfunction; Upregulation of Effective Neurogenesis with the Abrogated Apoptosis and Neuroinflammation. J. Mol. Neurosci. MN 56, 708–721. https://doi.org/10.1007/s12031-015-0492-y

Alvira-Botero, X., Carro, E.M., 2010. Clearance of amyloid-β peptide across the choroid plexus in Alzheimer's disease. Curr. Aging Sci. 3, 219–229.

Andersen, A.D., Binzer, M., Stenager, E., Gramsbergen, J.B., 2017. Cerebrospinal fluid biomarkers for Parkinson's disease – a systematic review. Acta Neurol. Scand. 135, 34–56. https://doi.org/10.1111/ane.12590

Baker, S.L., Maass, A., Jagust, W.J., 2017. Considerations and code for partial volume correcting [18F]-AV-1451 tau PET data. Data Brief 15, 648–657. https://doi.org/10.1016/j.dib.2017.10.024

Balusu, S., Brkic, M., Libert, C., Vandenbroucke, R.E., 2016. The choroid plexus-cerebrospinal fluid interface in Alzheimer's disease: more than just a barrier. Neural Regen. Res. 11, 534–537. https://doi.org/10.4103/1673-5374.180372

Bedussi, B., van Lier, M.G.J.T.B., Bartstra, J.W., de Vos, J., Siebes, M., VanBavel, E., Bakker, E.N.T.P., 2015. Clearance from the mouse brain by convection of interstitial fluid towards the ventricular system. Fluids Barriers CNS 12. https://doi.org/10.1186/s12987-015-0019-5

Benarroch, E.E., 2016. Choroid plexus--CSF system: Recent developments and clinical correlations. Neurology 86, 286–296. https://doi.org/10.1212/WNL.0000000000002298

Blennow, K., Hampel, H., Weiner, M., Zetterberg, H., 2010. Cerebrospinal fluid and plasma biomarkers in Alzheimer disease. Nat. Rev. Neurol. 6, 131–144. https://doi.org/10.1038/nrneurol.2010.4

Bolos, M., Antequera, D., Aldudo, J., Kristen, H., Bullido, M.J., Carro, E., 2014. Choroid plexus implants rescue Alzheimer's disease-like pathologies by modulating amyloid-β degradation. Cell. Mol. Life Sci. CMLS 71, 2947–2955. https://doi.org/10.1007/s00018-013-1529-4

Crossgrove, J.S., Li, G.J., Zheng, W., 2005. The choroid plexus removes beta-amyloid from brain cerebrospinal fluid. Exp. Biol. Med. Maywood NJ 230, 771–776.

Cserr, H.F., Cooper, D.N., Milhorat, T.H., 1977. Flow of cerebral interstitial fluid as indicated by the removal of extracellular markers from rat caudate nucleus. Exp. Eye Res., The Ocular and Cerebrospinal Fluids 25, 461–473. https://doi.org/10.1016/S0014-4835(77)80041-9

Damkier, H.H., Brown, P.D., Praetorius, J., 2013. Cerebrospinal fluid secretion by the choroid plexus. Physiol. Rev. 93, 1847–1892. https://doi.org/10.1152/physrev.00004.2013

Dangouloff-Ros, V., Grevent, D., Pagès, M., Blauwblomme, T., Calmon, R., Elie, C., Puget, S., Sainte-Rose, C., Brunelle, F., Varlet, P., Boddaert, N., 2015. Choroid Plexus Neoplasms: Toward a Distinction between Carcinoma and Papilloma Using Arterial Spin-Labeling. Am. J. Neuroradiol. 36, 1786–1790. https://doi.org/10.3174/ajnr.A4332

de Leon, M.J., Pirraglia, E., Osorio, R.S., Glodzik, L., Saint-Louis, L., Kim, H.-J., Fortea, J., Fossati, S., Laska, E., Siegel, C., Butler, T., Li, Y., Rusinek, H., Zetterberg, H., Blennow, K., Alzheimer's Disease Neuroimaging Initiative, National Alzheimer's Coordinating Center, 2018. The nonlinear relationship between cerebrospinal fluid Aβ42 and tau in preclinical Alzheimer's disease. PloS One 13, e0191240. https://doi.org/10.1371/journal.pone.0191240

Edsbagge, M., Andreasson, U., Ambarki, K., Wikkelsø, C., Eklund, A., Blennow, K., Zetterberg,

H., Tullberg, M., 2017. Alzheimer's Disease-Associated Cerebrospinal Fluid (CSF) Biomarkers do not Correlate with CSF Volumes or CSF Production Rate. J. Alzheimers Dis. JAD 58, 821–828. https://doi.org/10.3233/JAD-161257

Fujiyoshi, M., Tachikawa, M., Ohtsuki, S., Ito, S., Uchida, Y., Akanuma, S.-I., Kamiie, J., Hashimoto, T., Hosoya, K.-I., Iwatsubo, T., Terasaki, T., 2011. Amyloid-β peptide(1-40) elimination from cerebrospinal fluid involves low-density lipoprotein receptor-related protein 1 at the blood-cerebrospinal fluid barrier. J. Neurochem. 118, 407–415. https://doi.org/10.1111/j.1471-4159.2011.07311.x

Harrison, I.F., Siow, B., Akilo, A.B., Evans, P.G., Ismail, O., Ohene, Y., Nahavandi, P., Thomas, D.L., Lythgoe, M.F., Wells, J.A., 2018. Non-invasive imaging of CSF-mediated brain clearance pathways via assessment of perivascular fluid movement with diffusion tensor MRI. eLife 7. https://doi.org/10.7554/eLife.34028

Hong, Z., Shi, M., Chung, K.A., Quinn, J.F., Peskind, E.R., Galasko, D., Jankovic, J., Zabetian, C.P., Leverenz, J.B., Baird, G., Montine, T.J., Hancock, A.M., Hwang, H., Pan, C., Bradner, J., Kang, U.J., Jensen, P.H., Zhang, J., 2010. DJ-1 and alpha-synuclein in human cerebrospinal fluid as biomarkers of Parkinson's disease. Brain J. Neurol. 133, 713–726. https://doi.org/10.1093/brain/awq008

Iliff, J.J., Wang, M., Liao, Y., Plogg, B.A., Peng, W., Gundersen, G.A., Benveniste, H., Vates, G.E., Deane, R., Goldman, S.A., Nagelhus, E.A., Nedergaard, M., 2012. A Paravascular Pathway Facilitates CSF Flow Through the Brain Parenchyma and the Clearance of Interstitial Solutes, Including Amyloid β. Sci. Transl. Med. 4, 147ra111. https://doi.org/10.1126/scitranslmed.3003748

Jack, C.R., Holtzman, D.M., 2013. Biomarker Modeling of Alzheimer's Disease. Neuron 80, 1347–1358. https://doi.org/10.1016/j.neuron.2013.12.003

Jessen, N.A., Munk, A.S.F., Lundgaard, I., Nedergaard, M., 2015. The Glymphatic System: A Beginner's Guide. Neurochem. Res. 40, 2583–2599. https://doi.org/10.1007/s11064-015-1581-6

Krzyzanowska, A., Carro, E., 2012. Pathological Alteration in the Choroid Plexus of Alzheimer's Disease: Implication for New Therapy Approaches. Front. Pharmacol. 3. https://doi.org/10.3389/fphar.2012.00075

Landau, S.M., Lu, M., Joshi, A.D., Pontecorvo, M., Mintun, M.A., Trojanowski, J.Q., Shaw, L.M., Jagust, W.J., Alzheimer's Disease Neuroimaging Initiative, 2013. Comparing positron emission tomography imaging and cerebrospinal fluid measurements of β-amyloid. Ann. Neurol. 74, 826–836. https://doi.org/10.1002/ana.23908

Mawuenyega, K.G., Sigurdson, W., Ovod, V., Munsell, L., Kasten, T., Morris, J.C., Yarasheski, K.E., Bateman, R.J., 2010. Decreased clearance of CNS beta-amyloid in Alzheimer's disease. Science 330, 1774. https://doi.org/10.1126/science.1197623

Ott, B.R., Cohen, R.A., Gongvatana, A., Okonkwo, O.C., Johanson, C.E., Stopa, E.G., Donahue, J.E., Silverberg, G.D., Alzheimer's Disease Neuroimaging Initiative, 2010. Brain ventricular volume and cerebrospinal fluid biomarkers of Alzheimer's disease. J. Alzheimers Dis. JAD 20, 647–657. https://doi.org/10.3233/JAD-2010-1406

Perl, D.P., 2010. Neuropathology of Alzheimer's Disease. Mt. Sinai J. Med. N. Y. 77, 32–42. https://doi.org/10.1002/msj.20157

RR, S., 2003. Choroid plexus papilloma of the posterior third ventricle during infancy & childhood: Report of two cases with management morbidities. Neurol. India 51, 379.

Sachan, D., 2017. Choroid Plexus Papilloma Causing CSF Shunt Ascites: A Rare Presentation 2, 2.

Sämgård, K., Zetterberg, H., Blennow, K., Hansson, O., Minthon, L., Londos, E., 2010. Cerebrospinal fluid total tau as a marker of Alzheimer's disease intensity. Int. J. Geriatr. Psychiatry 25, 403–410. https://doi.org/10.1002/gps.2353

Schreiber, S., Landau, S.M., Fero, A., Schreiber, F., Jagust, W.J., Alzheimer's Disease

Neuroimaging Initiative, 2015. Comparison of Visual and Quantitative Florbetapir F 18 Positron Emission Tomography Analysis in Predicting Mild Cognitive Impairment Outcomes. JAMA Neurol. 72, 1183–1190. https://doi.org/10.1001/jamaneurol.2015.1633

Shi, Y., Li, X., Chen, X., Xu, Y., Bo, G., Zhou, H., Liu, Y., Zhou, G., Wang, Z., 2017. Imaging findings of extraventricular choroid plexus papillomas: A study of 10 cases. Oncol. Lett. 13, 1479–1485. https://doi.org/10.3892/ol.2016.5552

Tarasoff-Conway, J.M., Carare, R.O., Osorio, R.S., Glodzik, L., Butler, T., Fieremans, E., Axel, L., Rusinek, H., Nicholson, C., Zlokovic, B.V., Frangione, B., Blennow, K., Ménard, J., Zetterberg, H., Wisniewski, T., de Leon, M.J., 2015. Clearance systems in the brain—implications for Alzheimer disease. Nat. Rev. Neurol. 11, 457–470. https://doi.org/10.1038/nrneurol.2015.119

van Waalwijk van Doorn, L.J.C., Gispert, J.D., Kuiperij, H.B., Claassen, J.A.H.R., Arighi, A., Baldeiras, I., Blennow, K., Bozzali, M., Castelo-Branco, M., Cavedo, E., Emek-Savaş, D.D., Eren, E., Eusebi, P., Farotti, L., Fenoglio, C., Ormaechea, J.F., Freund-Levi, Y., Frisoni, G.B., Galimberti, D., Genc, S., Greco, V., Hampel, H., Herukka, S.-K., Liu, Y., Lladó, A., Lleó, A., Nobili, F.M., Oguz, K.K., Parnetti, L., Pereira, J., Picco, A., Pikkarainen, M., de Oliveira, C.R., Saka, E., Salvadori, N., Sanchez-Valle, R., Santana, I., Scarpini, E., Scheltens, P., Soininen, H., Tarducci, R., Teunissen, C., Tsolaki, M., Urbani, A., Vilaplana, E., Visser, P.J., Wallin, A.K., Yener, G., Molinuevo, J.L., Meulenbroek, O., Verbeek, M.M., 2017. Improved Cerebrospinal Fluid-Based Discrimination between Alzheimer's Disease Patients and Controls after Correction for Ventricular Volumes. J. Alzheimers Dis. JAD 56, 543–555. https://doi.org/10.3233/JAD-160668

Zhou, G., Hotta, J., Lehtinen, M.K., Forss, N., Hari, R., 2015. Enlargement of choroid plexus in complex regional pain syndrome. Sci. Rep. 5, 14329. https://doi.org/10.1038/srep14329

Figure legends

Figure 1: ChP segmentation. (A) Brain axial and coronal slices show ChP within lateral ventricles (Left and middle panels). **(B)** ChP is characterized by a monolayer of epithelial cells around a stroma with blood vessels (data from Allen Brain Human Atlas; http://www.brain-map.org/) (right panel)**. (C)** ChP segmentation (yellow color) from 3T Structural T1-weighted MRIs of a representative subject in ADNI and PPMI dataset **(D)** ChP volume for each diagnostic group in the ADNI (green) and PPMI (orange) cohorts. We performed one-way ANOVA followed by Tukey test to examine difference in ChP volume across diagnostic groups across both cohorts. AD showed larger ChP volume compared to other groups ($p<0.05$).

ChP: choroid plexus; HC: Healthy controls; SMC: individuals with significant memory concern; EMCI: early-mild cognitive impairment; LMCI: late-mild cognitive impairment; AD: Alzheimer's disease; PD: Parkinson's disease; ADNI: Alzheimer's Disease Neuroimaging Initiative; PPMI: Parkinson's Progression Markers Initiative

Figure 2: Principal component analysis of CSF proteins. To capture the highest amount of variance in CSF proteins, we applied principal component analysis in PPMI **(A)** and ADNI-2 **(D)**. Principal component score is computed by projecting each data point coordinate (red dot) onto the new component (red lines) (Left plots; for illustration purposes only two CSF proteins are shown). The first principal component explains around 60 percent of variance in CSF proteins in PPMI (**B**) and ADNI-2 (**E**). The insets show the loadings of first principal component. The scatter plots show partial correlation between ChP volume and first principal component, after correcting for age, sex, APOEε4 status, group, and cortical volume in PPMI (**C**) and ADNI (**F**).

ChP: choroid plexus; PPMI: Parkinson's Progression Markers Initiative; ADNI: Alzheimer's Disease Neuroimaging Initiative

Figure 3: Variance in CSF proteins explained by ChP volume for each diagnostic group in the ADNI and the PPMI datasets. For each CSF protein, we fitted two linear regression models. The first model included age, sex, APOE ε4, cortical volume and ChP volume as independent variables and the second model included age, sex, APOE ε4, and cortical volume as independent variables to predict the level of CSF protein. To measure the amount of variance explained by ChP volume, we then subtracted the adjusted R^2 of the second model from the first model. The error bars indicate the standard deviation of change of R^2 in 1000 bootstrapped samples. The two models were compared using F-test. The asterisk shows if the F-test was statistically significant ($p<0.01$).

HC: Healthy controls; SMC: individuals with significant memory concern; EMCI: early-mild cognitive impairment; LMCI: late-mild cognitive impairment; AD: Alzheimer's disease; PD: Parkinson's disease; ADNI: Alzheimer's Disease Neuroimaging Initiative; PPMI: Parkinson's Progression Markers Initiative

Figure 4: Cortical volume, ventricular volume and their associations with CSF proteins compared to ChP volume. Cortical volume was measured by summing volume of left and right cortices (blue). Ventricular volume was measured by summing volumes of lateral ventricles (yellow), inferior lateral ventricle horns, third and fourth ventricle (ChP segmentation is in red) **(A)**. ChP volume was correlated with cortical volume ($r \sim 0.14$) and ventricular volume ($r \sim 0.63$) **(B)**. ChP volume, ventricular volume and cortical volume were separately added to the model, which included age, sex, diagnostic group and APOEε4 status **(C)**. ChP: choroid plexus; PPMI: Parkinson's Progression Markers Initiative; ADNI: Alzheimer's Disease Neuroimaging Initiative.

Figure 5: Partial correlation between ChP volume and t-tau and p-tau in the Amyloid-positive and Amyloid-negative groups. Participants were divided into Amyloid-positive based on the AV45 SUVR at baseline (AV45>=1.11).

	ADNI					PPMI	
Group	**Control**	**SMC**	**EMCI**	**LMCI**	**AD**	**Control**	**PD**
Demographic Information							
Number of subjects	115	60	127	119	88	94	208
Mean age	73.4 ± 6.3	71.5 ± 5.4	71.3 ± 7.0	72.0 ± 7.8	74.6 ± 8.0	60.2 ± 11.3	61.4 ± 9.5
Number of male (%)	57 (49%)	25 (41%)	69 (54%)	60 (50%)	50 (56%)	67 (71%)	129 (69%)
APOE4 status (Homozygous/Heterozygous)	6, 24	0, 19	6, 47	21, 38	20, 40	2, 23	5, 51
CSF biomarkers (pg/ml)							
t-tau	241.9 ± 95.9	238.4 ± 91.7	254.3 ± 121.0	297.3 ± 130.0	379.3 ± 140.8	52.1 ± 29.9	44.1 ± 18.1
p-tau	22.2 ± 9.8	21.8 ± 9.8	24.1 ± 13.6	28.8 + /- 14.2	37.3 ± 14.9	18.9 ± 13.1	16.1 ± 9.5
Aβ	1404.2 ± 689.5	1358.5 ± 589.2	1176.9 ± 560.9	946.7 ± 483.4	717.2 ± 423.1	371.5 ± 93.1	375.2 ± 99.1
α-syn	-	-	-	-	-	2169.9 ± 1162.4	1855.4 ± 740.3
Brain Volumes (ml)							
Total Brain Volume	1504.8 ± 174.5	1516.1 ± 188.9	1516.3 ± 168.0	1529.3 ± 183.2	1557.0 ± 190.5	1528.4 ± 175.0	1586.1 ± 180.6
Cortical volume	435.4 ± 40.7	441.1 ± 42.5	436.5 ± 40.7	429.4 ± 39.9	409.5 ± 49.3	463.9 ± 45.4	468.8 ± 49.6
Ventricular volume	22.3 ± 10.4	20.3 ± 8.6	22.9 ± 11.6	26.6 ± 13.4	31.1 ± 12.7	28.6 ± 15.3	32.1 ± 20.2
ChP volume (Right + Left)	2.5 ± 0.6	2.5 ± 0.6	2.5 ± 0.6	2.6 ± 0.7	2.9 ± 0.5	2.4 ± 0.7	2.3 ± 0.7
Left ChP volume	1.3 ± 0.3	1.4 ± 0.4	1.4 ± 0.3	1.4 ± 0.4	1.6 ± 0.3	1.2 ± 0.3	1.2 ± 0.4
Right ChP volume	1.2 ± 0.3	1.1 ± 0.3	1.2 ± 0.3	1.2 ± 0.4	1.3 ± 0.2	1.1 ± 0.4	1.1 ± 0.3
PET imaging							
Florbetapir (AV45) (baseline)	1.12 ± 0.19	1.13 ± 0.17	1.17 ± 0.20	1.26 ± 0.24	1.39 ± 0.21	-	-
Amyloid positive (SUVR>= 1.11) (%)	39 (33%)	24 (40%)	61 (48%)	77 (64%)	78 (88%)	-	-

Table 1: Demographic information, levels of CSF proteins, and imaging data in the ADNI and PPMI datasets.

Note: ADNI: Alzheimer's Disease Neuroimaging Initiative; ChP: choroid plexus; ChP: choroid plexus; APOEε4: apolipoprotein E ε4 allele; AD: Alzheimer's disease; SMC: significant memory concern; EMCI: early-mild cognitive impairment; LMCI: late-mild cognitive impairment; t-tau: total-tau; p-tau: phosphorylated-tau; Aβ: amyloid-β

	t-tau		p-tau		Aβ		α-syn	
	Coefficient	**P**	**Coefficient**	**P**	**Coefficient**	**P**	**Coefficient**	**P**
PPMI								
Age	0.017	< 0.01	0.013	< 0.01	0.001	-	0.01	< 0.01
Sex (male)	0.01	-	0.05	-	-0.01	-	0.12	-
APOEε4	0.02	-	0.02	-	-0.16	< 0.01	-0.01	-
ChP volume (ml)	**-0.24**	**< 0.01**	**-0.1**	**-**	**-0.1**	**< 0.01**	**-0.24**	**< 0.01**
Cortical volume (ml)	0.51	-	1.09	-	0.79	0.01	0.3	-
Ventricular volume (ml)	-0.002	-	-0.006	< 0.01	0.001	-	-0.002	-
Group PD	-0.16	< 0.01	-	-	-	-	-0.14	< 0.01
ADNI								
Age	0.015	< 0.01	0.17	< 0.01	0.004	-		
Sex (male)	-0.24	-	-0.01	-	-0.06	-		
APOEε4	0.2	< 0.01	0.24	< 0.01	-0.42	< 0.01		
ChP volume (ml)	**-0.33**	**< 0.01**	**-0.34**	**< 0.01**	**-0.176**	**-**		
Cortical volume (ml)	0.0008	-	0.0009	-	0.00124	-		
Ventricular volume (ml)	-0.004	-	-0.004	-	-0.007	< 0.01		
Group SMC	-0.009	-	-0.01	-	-0.01	-		
EMCI	0.047	-	0.06	-	-0.08	-		
LMCI	0.197	< 0.01	0.23	< 0.01	0.23	< 0.01		
AD	0.47	< 0.01	0.53	< 0.01	-0.31	< 0.01		

Table 2: Multivariate analysis of CSF proteins in PPMI and ADNI-2. The coefficients (unstandardized) and p-values for each predictor.

Note: ADNI: Alzheimer's Disease Neuroimaging Initiative; ChP: choroid plexus; APOEε4: apolipoprotein E ε4 allele; AD: Alzheimer's disease; SMC: significant memory concern; EMCI: early-mild cognitive impairment; LMCI: late-mild cognitive impairment; t-tau: total-tau; p-tau: phosphorylated-tau; Aβ: amyloid-β

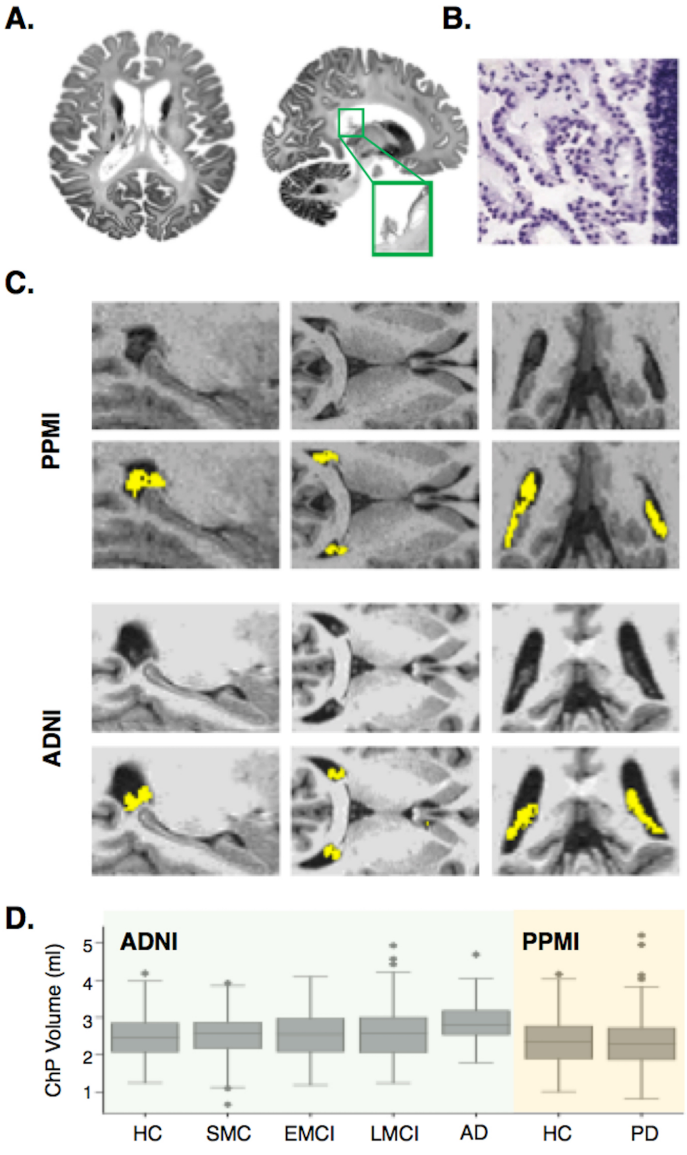
A.
B.
C.
PPMI
ADNI
D.
ADNI
PPMI
ChP Volume (ml)
5
4
3
2
1
HC
SMC
EMCI
LMCI
AD
HC
PD

PPMI

ADNI

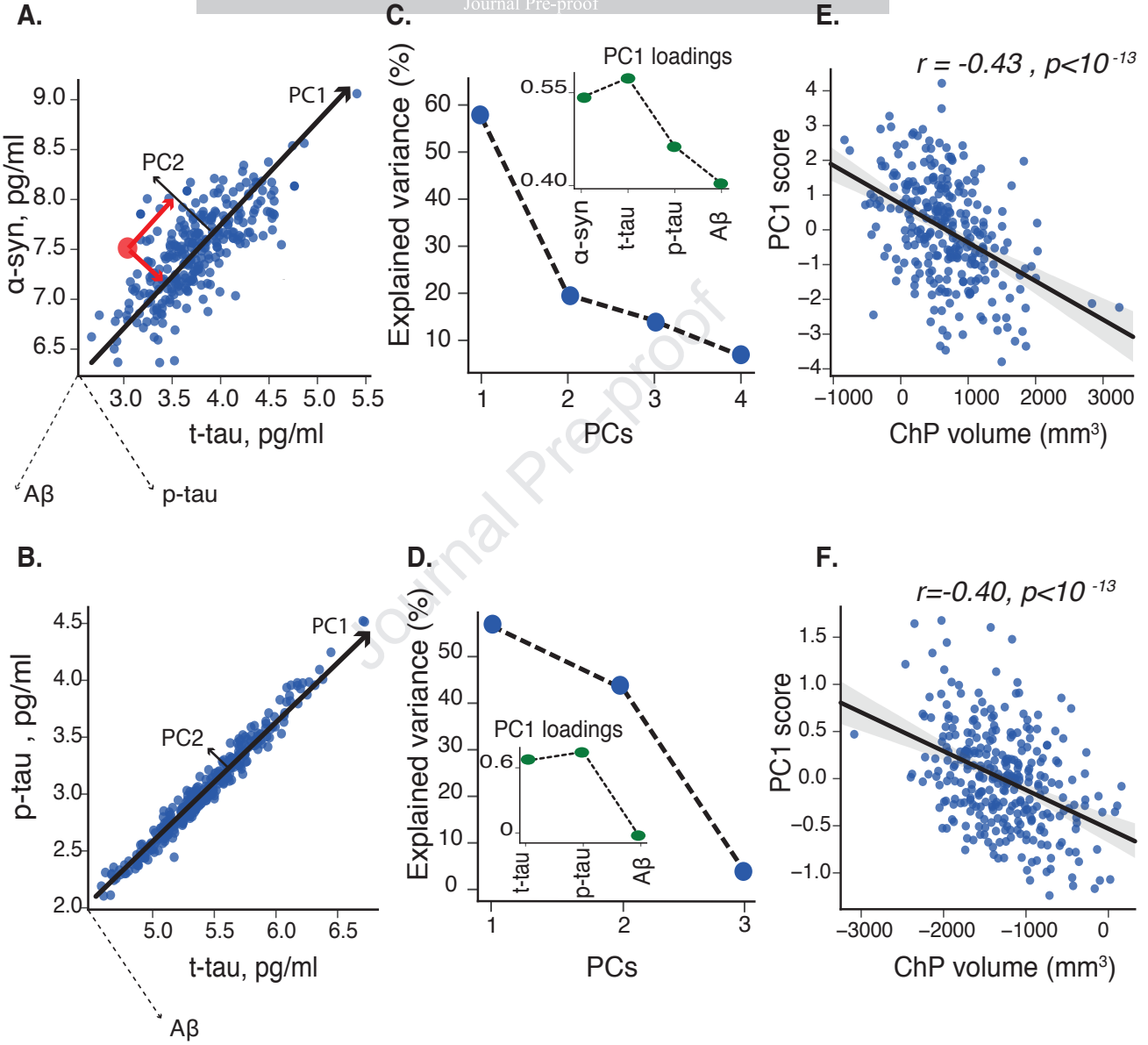

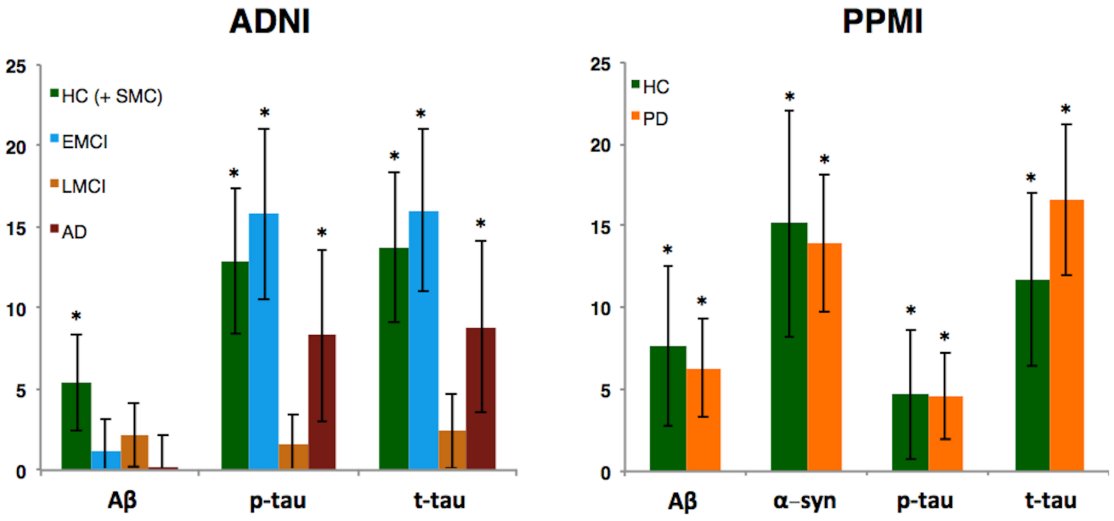

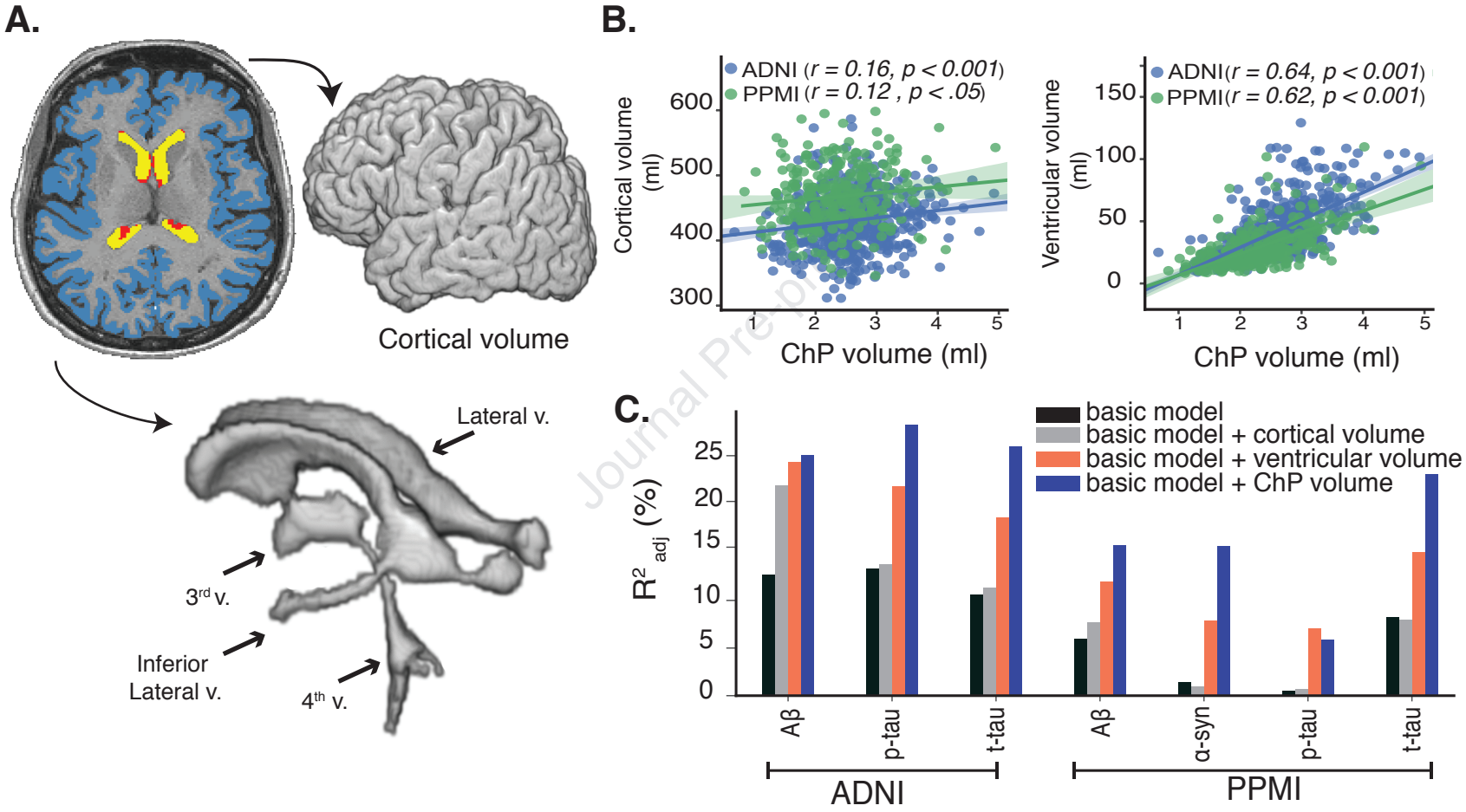

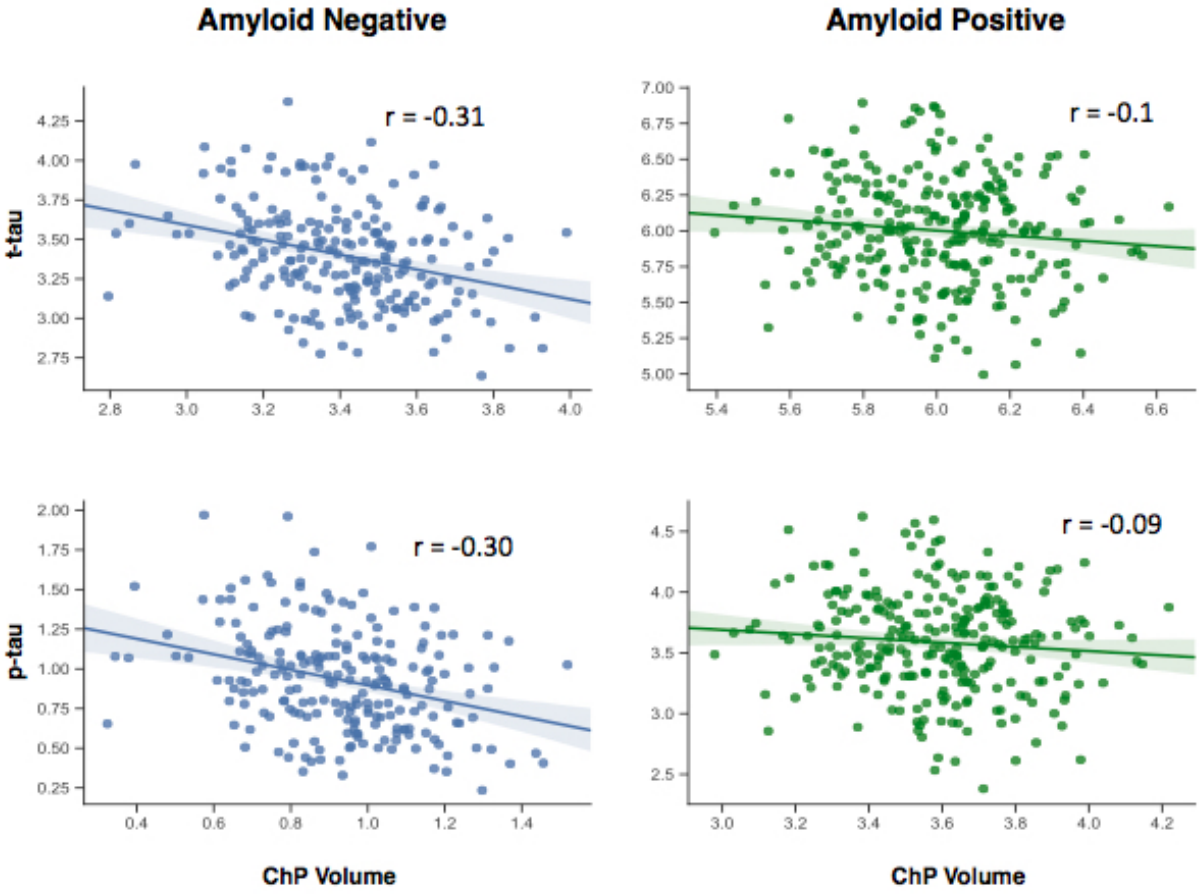
Amyloid Negative
Amyloid Positive
r = -0.31
r = -0.1
r = -0.30
r = -0.09
t-tau
p-tau
ChP Volume
ChP Volume

Highlights

- Negative associations exist between choroid plexus (ChP) volume and CSF-proteins.
- The negative association was lower in late mild cognitive impairment and AD patients.
- Florbetapir Amyloid-positive subjects had lower ChP volume/CSF-protein association.

The negative association between choroid plexus volume and CSF proteins declines in Alzheimer's disease but not Parkinson's disease

Ehsan Tadayon, M.D.[1], Alvaro Pascual-Leone, M.D., Ph.D.[2,3], Daniel Press, M.D.[1], Emiliano Santarnecchi, Ph.D.[1], for the Alzheimer's Disease Neuroimaging Initiative*

[1] *Berenson-Allen Center for Non-Invasive Brain Stimulation and Division for Cognitive Neurology, Beth Israel Deaconess Medical Center, Harvard Medical School, Boston, MA, USA*
[2] *Institut Universitari de Neurorehabilitacio Guttmann, Badalona, Barcelona, Spain*
[3] *Hinda and Arthur Marcus Institute for Aging Research and Center for Memory Health, Hebrew SeniorLife, Department of Neurology, Harvard Medical School, Boston, MA, USA*

*Data used in preparation of this article were obtained from the Alzheimer's Disease Neuroimaging Initiative (ADNI) database (adni.loni.usc.edu). As such, the investigators within the ADNI contributed to the design and implementation of ADNI and/or provided data but did not participate in analysis or writing of this report. A complete listing of ADNI investigators can be found at: http://adni.loni.usc.edu/wpcontent/uploads/how_to_apply/ADNI_Acknowledgement_List.pdf

Verifications

- We do not have related manuscripts on a similar topic submitted anywhere.
- All co-authors have reviewed and approved the present version for submission to the Neurobiology of Aging.
- Authors have no conflicts of interest to disclose.

Funding
ES and APL are supported by the BROAD Institute at Harvard-MIT (Boston, MA, USA) via 2016P000351. ES and APL are partially supported by Defense Advanced Research Projects Agency (DARPA) via HR001117S0030. ES is supported by the Beth Israel Deaconess Medical Center (BIDMC) via the Chief Academic Officer (CAO) grant 2017. APL is further supported by the Berenson-Allen Foundation, the Sidney R. Baer Jr. Foundation, grants from the National Institutes of Health (R01HD069776, R01NS073601, R21 MH099196, R21 NS082870, R21 NS085491, R21 HD07616), and Harvard Catalyst, The Harvard Clinical and Translational Science Center (NCRR and the NCATS NIH, UL1 RR025758). The content of this paper is solely the responsibility of the authors and does not necessarily represent the official views of Harvard Catalyst, Harvard University and its affiliated academic health care centers, the National Institutes of Health, the Sidney R. Baer Jr. Foundation.